

Ulysses observations of Microstreams in the Solar Wind from Coronal Holes

M. Neugebauer¹, B. E. Goldstein¹, D. J. McComas², S. T. Suess³, and A. Balogh⁴

¹ Jet Propulsion Laboratory, California Institute of Technology, Pasadena, CA 91109

² Los Alamos National Laboratory, Los Alamos, NM 87545

³ Marshall Space Flight Center, Huntsville, AL 35812

⁴ Imperial College, London, UK

Abstract

During its south polar passage in 1994, the Ulysses spacecraft continuously sampled the properties of the solar wind emanating from the south polar coronal hole. At latitudes poleward of $\sim 60^\circ$, the solar-wind speed had an average value of 764 km/s and a range of 700-833 km/s. The principal variations in the vector velocity were associated with either outward propagating Alfvén waves with periods up to about half a day or with longer-period high- or low-speed "microstreams". The microstreams had an amplitude of ~ 40 km/s and a mean half-width of 0.4 days, and they recurred on time scales of 2-3 days (power spectral peaks at 1.9 and 3.3 days). The density and temperature profiles showed the expected evidence of pileup and compression on the leading edges of high-speed microstreams, although no forward or reverse shocks were observed. The particle fluxes were nearly the same for both the fast and slow microstreams. The higher-speed microstreams had higher proton temperatures and higher alpha-particle abundances than did the slower microstreams. The absence of latitude variations in the thickness or the recurrence rate suggests that the microstreams are caused by temporal rather than long-lived ($>$ a few days) spatial variations in the source region at the Sun. Some speculations are made about the possible cause of the microstreams.

Introduction

Early near-Earth studies of the solar wind flow emanating from coronal holes indicated that many of the bulk plasma parameters, such as density, temperature, and speed were relatively constant [*Bame et al.*, 1977] while the vector velocity and vector magnetic field tended to vary because of the large amplitude of outward-propagating Alfvén waves [*Belcher and Davis*, 1971]. Helios data at heliocentric distances as small as 0.3 AU [*Thieme et al.*, 1988; 1990] provided evidence of variations of solar-wind density which were postulated to be related to variations of the source of the solar wind within the coronal holes; Thieme et al. suggested that the scale size of the density variations was consistent with modulation by the solar supergranulation structure. The long (nearly 2 year) continuous sampling of the flow of solar wind from the south polar coronal hole by the Ulysses spacecraft in 1993-5 provided the opportunity to study the substructures in coronal hole flow in detail. In surveying those data, *McComas et al.* [1995] found evidence for two types of density variations -- pileup at the leading edges of velocity gradients and other structures in which balance between thermal and magnetic pressures was maintained. This paper focuses on the velocity structures discussed by McComas et al. Following some precedents, we call them "microstreams". As part of the long-term objective of understanding the mechanisms responsible for the acceleration of the solar wind, we want to know the scale sizes of the microstreams, whether they are predominantly spatial or temporal in nature, and the relation of other solar-wind parameters (e.g., helium abundance, temperature, ion fluxes, plasma β , etc.) to the rises and falls in velocity. Such data are required to be able to model, and eventually to understand, which parameters are important in determining the end state of the acceleration process.

Data Set Used

The data used in this study were obtained by the Ulysses spacecraft during its out-of-the-ecliptic trajectory during 1994 when Ulysses covered a heliocentric distance range of 3.8 to 1.6 AU and a latitude range of -48 to -80° and then back to -45 . The plasma data were obtained by the Ulysses solar wind plasma experiment named Solar Wind Observations Over the Poles of the Sun (SWOOPS). The design and operation of SWOOPS are described by *Bame et al. [1992]*. In its usual mode of operation, SWOOPS measures the three-dimensional distribution of protons and alphas with spacings of 5% in energy, -5° in both polar and azimuthal angles, and either 4 or 8 minutes in time, depending on whether the spacecraft is being tracked or is storing data for later readout. SWOOPS obtains electron distributions every 5.7 or 11.3 minutes, and the electron data have been interpolated to match the times of ion observations. The magnetic field data were obtained by the Ulysses magnetometer [*Balogh et al., 1992*].

Figure 1 summarizes the velocity data obtained between Jan 1 and Dec 23, 1994. It is a stack-plot of 12-hour averages of the proton speed, with the data for each 25.5-day rotation starting 100 km/s above the data for the previous rotation. The day number at the start of each rotation is given at the left and the heliographic latitude at the end of the rotation is given at the right. The first four rotations show a recurring low speed interval between rotation days 15 and 18. Tracing the wind back to the Sun based on the assumption that the velocity is constant between the Sun and the point of measurement indicates that the lower speed wind originated at solar longitudes in the range 80 - 100° . Solar maps show the boundary of the south polar coronal hole at these longitudes to be well poleward of its average position. Thus Ulysses was probably closer to the low-latitude boundary of the flow from the polar coronal hole, i.e., less far into the hole, during the times when the lower speeds were observed. We note that this relation

between solar wind speed and distance from the coronal hole boundary is opposite to that predicted by *Wang and Sheeley* [1990].

Figure 1 also shows that the speed profile across a solar rotation was relatively flat starting at -Day 153 (latitude -66.3°) and continuing through Day 331 (latitude -61.60°), showing mostly small peaks and valleys of only a few days duration. In a study of **compressional** and **rarefaction** waves in the high-latitude solar wind, *Phillips et al. [1995]* also came to the conclusion that the effects of modulation caused by solar rotation and the tilt of the solar dipole field died away at $\sim 60^\circ$ latitude. The seven rotations poleward of -68° indicated by a vertical line at the right side of Figure 1 form the basis of the data set used in the present study. There have been no reports of solar wind associated with coronal mass ejections **during** that period.

Observational Results

Some of the velocity variations **observed** in the plasma from the south polar coronal hole are caused by the propagation of **Alfvén** waves away from the Sun [Goldstein et al., 1995; *Smith et al.*, 1995]. The relative importance of waves and variations caused by changes in the solar wind acceleration processes depends on the frequency of the variations. Figure 2 displays power spectra computed from hourly averages of each of the three components of the proton velocity during the 7-rotation **period** of interest. The power in the radial (R) **component** exceeds that in the tangential (T) and normal (N) components for periods greater than ~ 12 hours to one day ($f = 1.16 - 2.3 \times 10^{-5}$ Hz). In polar regions, where the spiral winding of the field is less than it is in equatorial regions, **Alfvén** waves should lead to fluctuations in the T and N components which equal or exceed those in the R component. Thus **Figure 2** can be interpreted as evidence that at periods greater than about half a day, the variations in V_R are largely intrinsic to the flow rather than caused by **Alfvén** waves. Figure 3 is consistent with this interpretation. It

shows a plot of the coherence between (5-point smoothed) hourly averages of B_R and V_R versus frequency. The high coherence expected for **Alfvén** waves is evident at frequencies above a few times 10^{-5} Hz, but is much less for periods greater than 12 hours.

The properties of the plasma in the peaks and valleys of the velocity profile are investigated using a superposed epoch analysis based on 6-hour averages of many plasma and field parameters. An averaging **interval** of 6 hours was selected to avoid most of the variations caused by **Alfvén** waves while still obtaining sufficient resolution with respect to the time scale of the rises and falls in velocity. Plots of 6-hour averages of proton speed versus time were scanned to select the times of the centers of 29 velocity peaks and the times of the centers of 17 velocity dips. The average values of several plasma parameters were then calculated for **five** 6-hour intervals on either side of the central peak and dip times. Some of the results are shown in **Figure 4**, with the variations around the velocity peaks shown on the left and the variations of the same parameters around the dips shown on the right.

Proton speed is plotted in the top panels. Not surprisingly, the average peak speed exceeds **the** average dip speed; the difference is 50 km/s. The error bars denote the standard error, which is the standard deviation divided by $(N - 1)^{1/2}$, where N is the number of points included in the average (either 29 or 17). The curves show some asymmetry, being steeper **before the peak and** after the dip, as expected by compression on the leading edges of fast streams. The superposition process has smoothed out some of this effect with many individual streams showing much stronger asymmetries (e.g., see Figure 2 of *McComas et al, [1995]*).

The second and third panels show the proton flux and the **proton** temperature, respectively, normalized to 1 AU. An inverse, square dependence on **heliocentric** distance was assumed for the normalization of the flux. For temperature, a least-squares, **power-law** fit of the 6-hour averages for these 7 solar rotations resulted in a dependence of $r^{-0.51}$,

which was used to **normalize** the temperatures to 1 AU before performing the superposition of the data. Both the flux and **the** temperature are highest when dV/dt is positive (before the peaks and after the dips) and lowest when dV/dt is negative (after the peaks and before **the** dips). This behavior is readily explained by the well known **compressional** pileup at the leading edges of high-speed streams where fast **plasma** is overtaking slower plasma in its path and **rarefactions** on the trailing edges where fast plasma is running away from the slower plasma **behind** it. Several specific examples of this phenomenon associated with **microstreams** in the polar coronal hole flow are shown by *McComas et al.* [1995].

What is more interesting about these two panels is the relative values at the peaks and dips themselves. The normalized proton flux at the peaks of the **microstreams** is the same as the flux at the bottoms of the dips, namely $1.9 \times 10^8 \text{ cm}^{-2} \text{ s}^{-1}$. The temperatures, however, are not the same, being a factor of 1.12 higher at the peaks than at the dips. Long-term averages of the near-ecliptic solar wind flow consistently show that the proton temperature increases with roughly the square of the speed [*Burlaga and Ogilvie, 1970; 1973*]. The Ulysses data **reveal** that the same relation holds for the **microstreams** within the flow from a polar coronal hole; a 6% increase in average speed between the peaks and dips is accompanied by a **12%** increase in **proton** temperature.

The fourth panels in Figure 4 show the superposed epoch data for the flux of alpha particles relative to the flux of protons. There appears to be a significant systematic variation through the peaks and dips, There is a regular pattern **across** the velocity structures with an average ratio of 0.047 ± 0.001 at the peaks and 0.040 ± 0.001 at the dips, Although a positive correlation between helium abundance and solar-wind speed has been known for several decades, it is now **known** that the lowest helium abundances are found in the low speed wind surrounding the **heliospheric** current sheet [*Borrini et al., 1981*] while the highest values are found in the transient flows from coronal mass ejections [*Hirshberg et al., 1972; Borrini et al., 1982.*]. *Bame et al.* [1977] commented on

the remarkable constancy of the helium abundance in (near-ecliptic) coronal hole flow. *Neugebauer [1992]*, on the other hand, found evidence that the faster a coronal-hole stream, the greater its average helium abundance. The velocity dependence of the helium abundance derived from Figure 4 above is much steeper than that reported by *Neugebauer [1992]* for stream-averaged data.

The bottom two sets of panels in Figure 4 show the behavior of the magnitude of the differential streaming between the alphas and protons, $V_{\alpha p}$, and the normalized cross helicity parameter σ_c defined as

$$\sigma_c = \frac{2\langle \delta V \cdot \delta B \rangle}{\langle \delta V^2 + \delta B^2 \rangle} \quad (1)$$

The averages indicated by the $\langle \rangle$ in (1) were taken over the individual spectra obtained within each of the 6-hour intervals contributing to the superposed epoch analysis. If the velocity and field variations were caused by purely outward propagating **Alfvén** waves, σ_c would equal 1.0. The decrease in σ_c in the compression regions in front of the peaks and behind the dips is probably caused by the plasma interactions which can generate additional wave modes. These interactions also apparently disrupt or limit the differential streaming between the alphas and protons, resulting in $V_{\alpha p}$ being greatest at the **rarefaction** parts of the profiles.

The parameters T_{\parallel}/T_{\perp} for protons, the electron temperature T_e , the magnetic field strength B , and plasma $\beta = 8\pi(nkT)/B^2$ were also examined in the format of Figure 4, but revealed no consistent patterns relative to the peaks and dips. Superposed-epoch plots of the flow directions showed the diversion of the ambient plasma in the interaction regions already discussed by *McComas et al. [1995]*.

A question that naturally arises is whether the microstreams are caused by spatial or by temporal structures in the corona? A hint can be found in the latitude dependence of the duration of the microstreams as seen at Ulysses. If the microstreams are long-lived

compared to their observed durations and have a uniform size distribution throughout the polar coronal hole, the time required for each of them to corotate past the spacecraft should increase with latitude λ as $1/\cos\lambda$, with the limiting case of a spacecraft at $\lambda = 90^\circ$ being in a polar microstream continuously. Figure 5 displays the mean widths w of the peaks and dips selected for the superposed epoch analysis plotted versus heliographic latitude. The mean width is defined by

$$w = \frac{\sum (V_i - V_0)(t_i - \langle t \rangle)}{\sum (V_i - V_0)} \quad (2)$$

where the sum is taken over nine 6-hour intervals centered on each peak or dip, V_i is the speed during the i th interval, and V_0 is the minimum (or maximum) value of the nine values of V_i surrounding the peak (or the dip). Figure 5 shows no clear dependence of the peak width on latitude. Note that the function $1/\cos\lambda$ would more than double between 65° and 80° . Unfortunately, the data used to construct Figure 5 may be subject to a bias introduced in the selection of the peaks and dips for the superposition analysis; neither very broad, overlapping or complex structures nor extremely narrow structures were selected.

An alternative technique is to compute power spectra of the variations in speed for data taken over different latitude ranges. The results are shown in Figure 6, where each power spectrum was computed from 64-days of data, the first preceding the ‘‘polar’’ passage ($\lambda = -65.8^\circ$ to -75.8°), the second at the highest latitudes ($\lambda = -75.8^\circ$ to -80.2° , and then back to -78.4°) and the third on the equatorward part of the trajectory ($\lambda = -78.4^\circ$ to -56.9°). The value of $1/\cos\langle\lambda\rangle$ for each of the three intervals is 3.02, 5.21, and 2.78, respectively. The spectral peaks at 1.9 and 3.3 days (marked by vertical lines in Figure 6) remain at the same frequencies for all three intervals; there is no indication of a shift to lower frequency (longer periods) for the second (highest-latitude) interval. The error bar in Figure 6 shows* the mean error corresponding to the 10 degrees of freedom in each

power spectrum. This error is sufficiently large that some of the peaks, especially in the third interval, are of questionable statistical significance. It is noted that the apparent systematic decrease in low-frequency power from interval 1 to interval 3 is not a general result; examination of the intervals before and after the three selected intervals do not continue that trend.

Discussion

In an earlier paper *McComas et al. [1995]* described some of the features of temporal variations in the high-speed flow from the Sun's south polar coronal hole. They found two types of features -- those characterized by changes in speed (which we call microstreams) and those characterized by pressure balance and changes in β . Additional properties of high- and low-speed microstreams have been described in the previous section. They have an amplitude of ~ 40 km/s and a half-width of 0.4 days and they recur on time scales of 2-3 days. They show the classic signatures of compression and rarefaction on their leading and trailing edges, respectively. The faster microstreams have higher temperatures and higher helium abundances than do the slower ones which correspond to dips in the speed profile. Despite the lack of statistically incontrovertible evidence that the duration and recurrence rate of the microstreams remain nearly constant with latitude, we can find no evidence to the contrary. One possible interpretation of this result is that the microstreams become physically narrower with increasing latitude approximately as $1/\cos\lambda$. Not only does such a scenario seem improbable, but coronagraph and eclipse images show no latitudinal narrowing of features such as polar plumes. We therefore conclude that the microstreams are probably a temporal phenomenon, with each stream enduring no more than a few days.

The microstreams were observed at all heliocentric distances between 3 and 1.8 AU as Ulysses moved through the high-latitude wind from the polar coronal hole. Why hadn't

stream-stream interactions on the leading edges wiped out the gradients at smaller distances? One way to estimate the distance at which nonlinear interactions become important is by applying the formula for the intersection of characteristics [Steinolfson, 1985]:

$$\Delta\tau_i = \frac{l\Delta V}{(C_f + V)(C_f + V + \Delta V)} \quad (3)$$

where C_f is the ambient fast-mode wave speed and l is the heliocentric distance at which a shock will form if the velocity is increased by an amount ΔV above the ambient speed V over a time $\Delta\tau_i$. Table 1 presents the values of l calculated for each of three 10-day intervals included in the present study. For the calculations it was assumed that $\Delta\tau_i = 0.37$ days (the average value of w shown in Figure 5) and $\Delta V = 40$ km/s, consistent with Figure 4. For the high-latitude **microstreams**, however, shock formation is not really expected; instead the **streams are** believed to interact, produce transverse flow, and eventually evolve into a spectrum of turbulent eddies. But the fact that the values of l displayed in Table 1 are significantly larger than the distances at which the microstreams were observed indicates that the interactions are not expected to have proceeded very far by the point of observation.

The principal mystery concerning the microstreams is their cause. There is no obvious coronal feature with the required temporal and spatial properties. The absence of a latitude signature in the duration and the recurrence rate of the **microstreams** rules out an origin in long-lived **corotating** structures. At the **other** extreme, **the** data do not rule out global temporal oscillations with a 2 or 3 day period, In Thomson's (D. J. Thomson, personal communication) analysis of **Ulysses** **energetic** it-particle and magnetic-field data, two of the 19 frequencies observed in at least 7 data sets had **periods** of 1.9 and 3.3 days, in agreement with Figures 2 and 6. We do not know what causes those periodicities. The high density of solar g-mode frequencies in that frequency range makes it difficult to

understand why those two particular frequencies would be excited in preference to neighboring frequencies if global g-mode oscillations were the cause.

Suppose the **microstreams** are caused by **corotating** structures with lifetimes of 2-3 days. In such a scenario, the beams of plasma with speeds higher or lower than average must be spatially wide enough that they do not **corotate** past Ulysses in less than about a day. At a latitude of **60°**, this requirement sets a lower limit on the scale size (full width) of the sources of the **microstreams** of $\sim 10^4$ km.

Aside from very long-lived streamers, which are not candidate sources for microstreams, the only known structures to extend beyond a few solar radii are the polar plumes seen in eclipse or coronagraph images. Individual plumes have lifetimes of several hours to several days, with an average of 15 hours, and their mean half width is $\sim 3.3 \times 10^4$ km [Newkirk and Harvey, 1968]. Although both the average duration and the average width of the plumes are slightly less than the values calculated above for the microstream source, the differences are not great enough to eliminate a possible relation between plumes and **microstreams**.

Perhaps a more serious difficulty with relating the **microstreams** to polar plumes involves the properties of the **microstreams** other than their velocity profiles. A recent model of the acceleration of the solar wind in coronal holes by *Habbal et al.* [1995] indicates that higher coronal densities such as might be associated with polar plumes are expected to be associated with decreases in solar wind speed and with increases in the proton temperature and alpha-particle abundance. These results are the opposite of those found in this study -- namely that higher temperatures and alpha abundances are found in the faster, rather than in the slower **microstreams**. A model of polar plumes by *Wang* [1994] also yields correlations different from those observed; Wang's model plumes have higher fluxes and lower speeds at 1 AU than does the **interplume** wind, whereas the microstreams observed by Ulysses show no correlation between velocity and flux. Finally, it is generally thought that polar plumes are controlled by the magnetic structure

in the corona, but we found no systematic relation between magnetic properties such as field strength or plasma β and the **microstreams**. The pressure-balance structures observed by Ulysses [*McComas et al.*, 1995] may be more closely related to polar plumes than are the **microstreams** defined by the velocity profiles.

An alternative possibility is that the **microstreams** are caused by impulsive events rather than by corotating structures. Acceleration of a gram of solar wind plasma from 750 to 790 **km/s** requires 3×10^{14} erg. According to *Brueckner and Bartoe [1983]*, a large coronal jet event provides 3×10^{26} erg to 3×10^{11} gm, or 10^{15} erg/gm, which is a factor of 3 more than required to explain the excess energy in the **microstreams**. From an observation of jets in coronal holes, *Brueckner and Bartoe* estimate a whole-Sun occurrence rate for large jets of 5 S-1. For Ulysses to detect only one of those events every 3 days requires connection to a source region with a diameter of 2400 km, which compares remarkably well with the 3000 km size of large jets. It might be possible, however, that localized impulses in coronal holes, such as jets or flaring bright points, propagate throughout the hole instead of affecting just a small stream tube. In that case the appropriate occurrence rate would be the rate averaged over the entire hole, which is much greater than the observed frequency of **microstreams**. In short, there is no good physical model to relate coronal jets to **microstreams**.

In conclusion, we don't know what causes **microstreams**. The speculations about plumes and jets given above do not cover all possibilities and much more work is required to see what makes sense,

Acknowledgments. We thank David J. Thomson for information about the frequencies observed in the energetic particle and magnetic field data. Discussions with Roger **Ulrich** and **Shadia Habbal** were also very helpful in trying to understand possible solar aspects of the Ulysses observations. We gratefully acknowledge the work of the Los Alamos group who built the SWOOPS instrument under the guidance of the original

Principal Investigator Sam J. Bame. Regina Sakurai's assistance with the data reduction was also invaluable. This paper presents the results of research performed at the Jet Propulsion Laboratory of the California Institute of Technology under contract to NASA. The work at Los Alamos was performed under the auspices of the US Department of Energy with financial support from NASA.

Table 1. Ten-day averages of heliographic latitude λ and distance R, fast-mode wave speed C_f , solar wind speed V, and steepening distance l as calculated from Equation (3).

Days, 1994	λ , deg	R, AU	C_f , km/s	V, km/s	l , AU
153-163	-67	2.95	61	769	3.9
250-260	-80	2.30	76	760	3.9
322-332	-64	1.80	69	735	3.6

REFERENCES

- Balogh, A., T. J. Beck, R. J. Forsyth, P. C. Hedgecock, R. J. Marquedant, E. J. Smith, D. J. Southwood, and B. T. Tsurutani, The magnetic field investigation on the Ulysses mission: instrumentation and preliminary scientific results, *Astron. Astrophys. Suppl.*, 92,221, 1992.
- Bame, S. J., J. R. Asbridge, W. C. Feldman, and J. T. Gosling, Evidence for a structure-free state at high solar wind speeds, *J. Geophys. Res.*, 82, 1487, 1977.
- Bame, S. J., D. J. McComas, B. L. Barraclough, J. L. Phillips, K. J. Sofaly, J. C. Chavez, B. E. Goldstein, and R. K. Sakurai, The Ulysses solar wind plasma experiment, *Astron. and Astrophys. Suppl.*, 92,237, 1992.
- Belcher, J. W., and L. Davis, Jr., Large-amplitude Alfvén waves in the interplanetary medium, *J. Geophys. Res.*, 76, 3534, 1971.
- Borrini, G., J. T. Gosling, S. J. Bame, and W. C. Feldman, Helium abundance enhancements in the solar wind, *J. Geophys. Res.*, 87,7370, 1982.
- Borrini, G., J. T. Gosling, S. J. Bame, W. C. Feldman, and J. M. Wilcox, Solar wind helium and hydrogen structure near the heliospheric current sheet: a signal of coronal streamers at 1 AU, *J. Geophys. Res.*, 86, 4565, 1981.
- Brueckner, G. E., and J.-D. F. Bartoe, Observations of high-energy jets in the corona above the quiet sun, the heating of the corona, and the acceleration of the solar wind, *Astrophys. J.*, 272,329, 1983.
- Burlaga, L. F., and K. W. Ogilvie, Heating of the solar wind, *Astrophys. J.*, 159,659, 1970.
- Burlaga, L. F., and K. W. Ogilvie, Solar wind temperature and speed, *J. Geophys. Res.*, 78,2028, 1973.
- Goldstein, B. E., M. Neugebauer, and E. J. Smith, Alfvén waves, alpha particles, and pickup ions in the solar wind, *Geophys. Res. Lett.*, Submitted, 1995.

- Habbal, S. R., R. Esser, M. Guhathakurta, and R. Risher, Flow properties of the solar wind derived from a two-fluid model with constraints from white light and interplanetary data, *Geophys. Res. Lett.*, In press, 1995.
- Hirshberg, J., S. J. Bame, and D. E. Robbins, Solar flares and solar wind helium enrichments: July 1965-July 1967, *Sol. Phys.*, 23,467, 1972.
- McComas, D. J., B. L. Barraclough, J. 'T. Gosling, C. M. Hammond, M. Neugebauer, A. Balogh, and R. Forsyth, Structures in the polar solar wind: plasma and field observations from Ulysses, *J. Geophys. Res.*, in press, 1995.
- Neugebauer, M., Knowledge of coronal heating and solar-wind acceleration obtained from observations of the solar wind near 1 AU, in *Solar Wind Seven*, edited by E. Marsch and R. Schwenn, pp. 69, Pergamon Press, Oxford, 1992.
- Newkirk, G., and J. Harvey, Coronal polar plumes, *Solar Phys.*, 3,321, 1968.
- Phillips, J. L., B. E. Goldstein, J. T. Gosling, C. M. Hammond, J. T. Hoeksema, and D. J. McComas, Sources of solar wind shocks and compressions at high solar latitudes: Ulysses, *Geophys. Res. Lett.*, Submitted, 1995.
- Smith, E. J., M. Neugebauer, A. Balogh, S. J. Bame, R. P. Lepping, and B. T. Tsurutani, Ulysses observations of latitude gradients in the heliospheric magnetic field: radial component and variances, *Space Sci. Rev.*, 72, 165, 1995.
- Steinolfson, R. S., Theories of shock formation in the solar atmosphere, in *Collisionless Shocks in the Heliosphere: Reviews of Current Research; Geophysical Monograph 35*, edited by B. Tsurutani and R. G. Stone, pp. 1, Amer. Geophys. Un., Washington, DC, 1985.
- Thieme, K. M., E. Marsch, and R. Schwenn, Relationship between structures in the solar wind and their source regions in the corona, in *Proceedings of the Sixth International Solar Wind Conference, NCAR/TN-306+Proc*, edited by V. J. Pizzo, T. E. Holzer and D. G. Sime, pp. 317, National Center for Atmospheric Research, Boulder, CO, 1988.

Thieme, K. M., E. Marsch, and R. Schwenn, Spatial structures in high-speed streams as signatures of fine structures in coronal holes, *Ann. Geophys.*, 8,713, 1990.

Wang, Y.-M., Polar plumes and the solar wind, *Astrophys. J.*, 435,1.153, 1994,

Wang, Y.-M., and J. N. R. Sheeley, Solar wind speed and coronal flux-tube expansion, *Astrophys. J.*, 355,726, 1990.

Figure Captions

Fig. 1. Stack plot of 12-hour averages of the solar wind speed observed by Ulysses during 1994. The data for each solar rotation period (as observed from Ulysses) are placed 100 km/s above the data for the previous rotation. Day numbers at the beginning of each rotation are given at the left while the heliographic latitudes at the end of each rotation are given at the right.

Fig. 2. Power spectra of the radial (R), tangential (T), and normal (N) components of the solar-wind proton velocity for the seven solar rotations marked by a bar on the right side of Figure 1. Hourly average values were used to compute the spectra,

Fig. 3. The coherence between V_R and B_R as a function of frequency for the power spectrum shown in Figure 2.

Fig. 4. Superposed epoch analysis of 6-hour averages of various plasma parameters observed by Ulysses. The zero times were selected to fall on local maxima (Peak) or local minima (Dip) of the solar-wind speed profile. See text for discussion of the parameters plotted.

Fig. 5. The mean width, in days, of the peaks and dips used in the superposed epoch analysis plotted versus heliographic latitude at the time of observation.

Fig. 6. Power spectra of the radial component of the proton velocity for three 64-day intervals with the mean latitudes and heliocentric distances identified in the box.

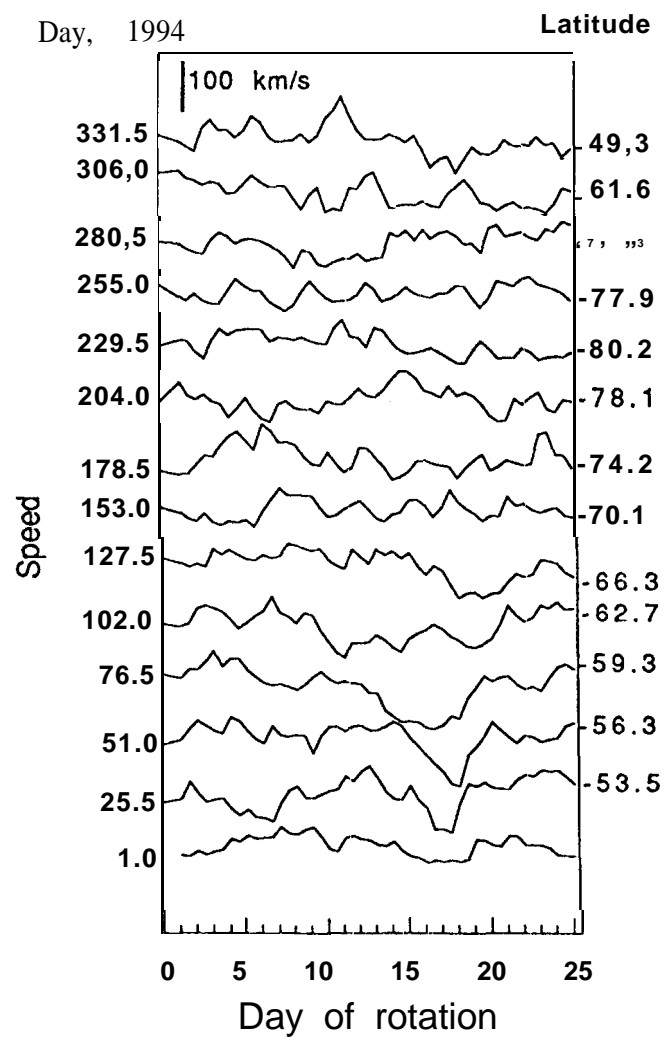


Fig. 1

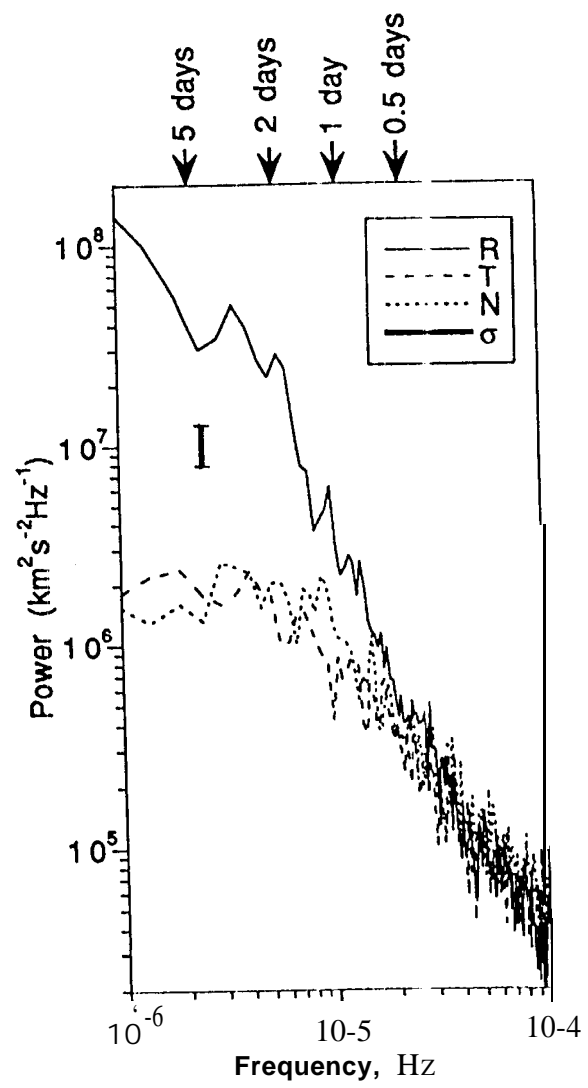


Fig 2

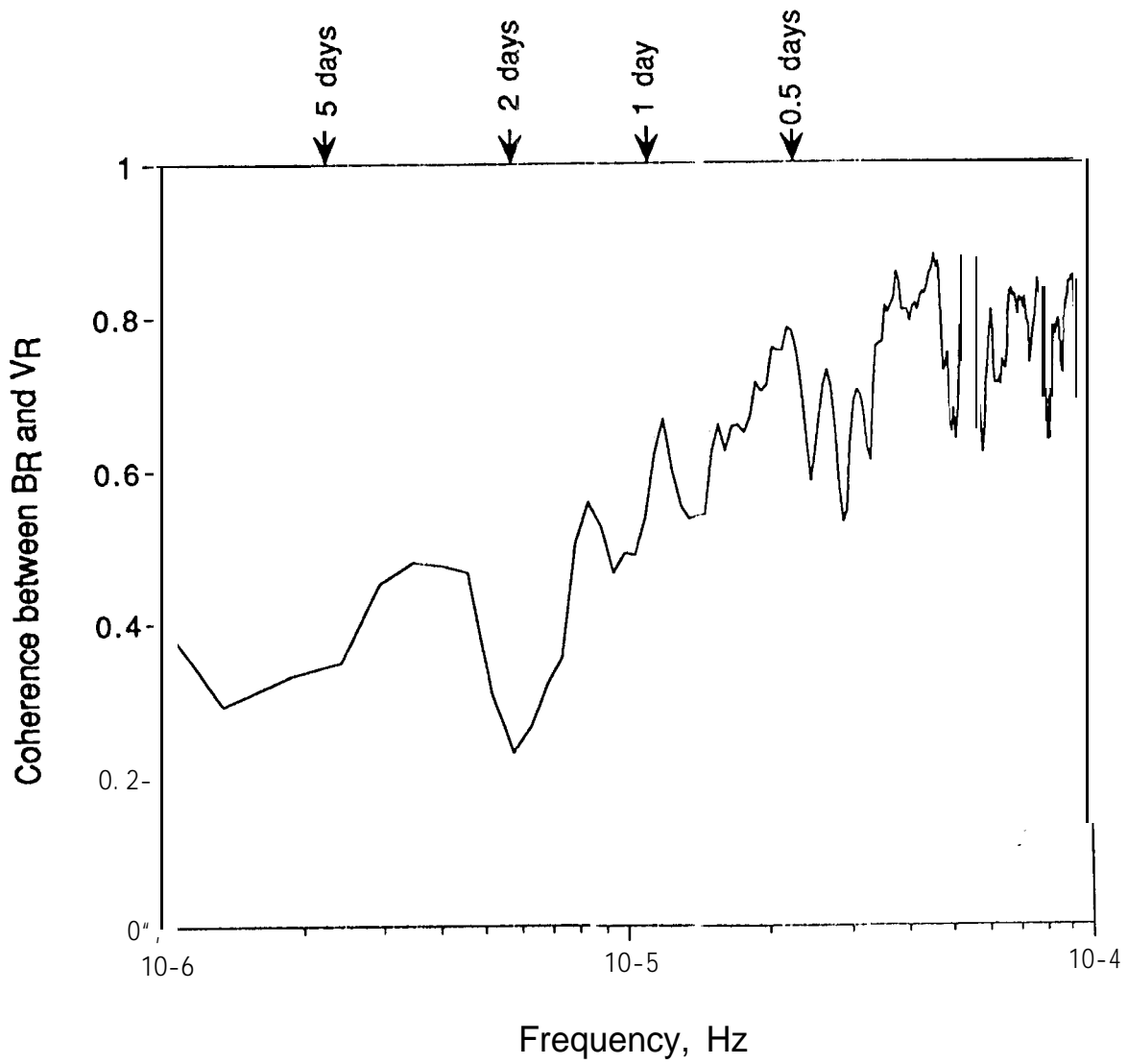


Fig. 3

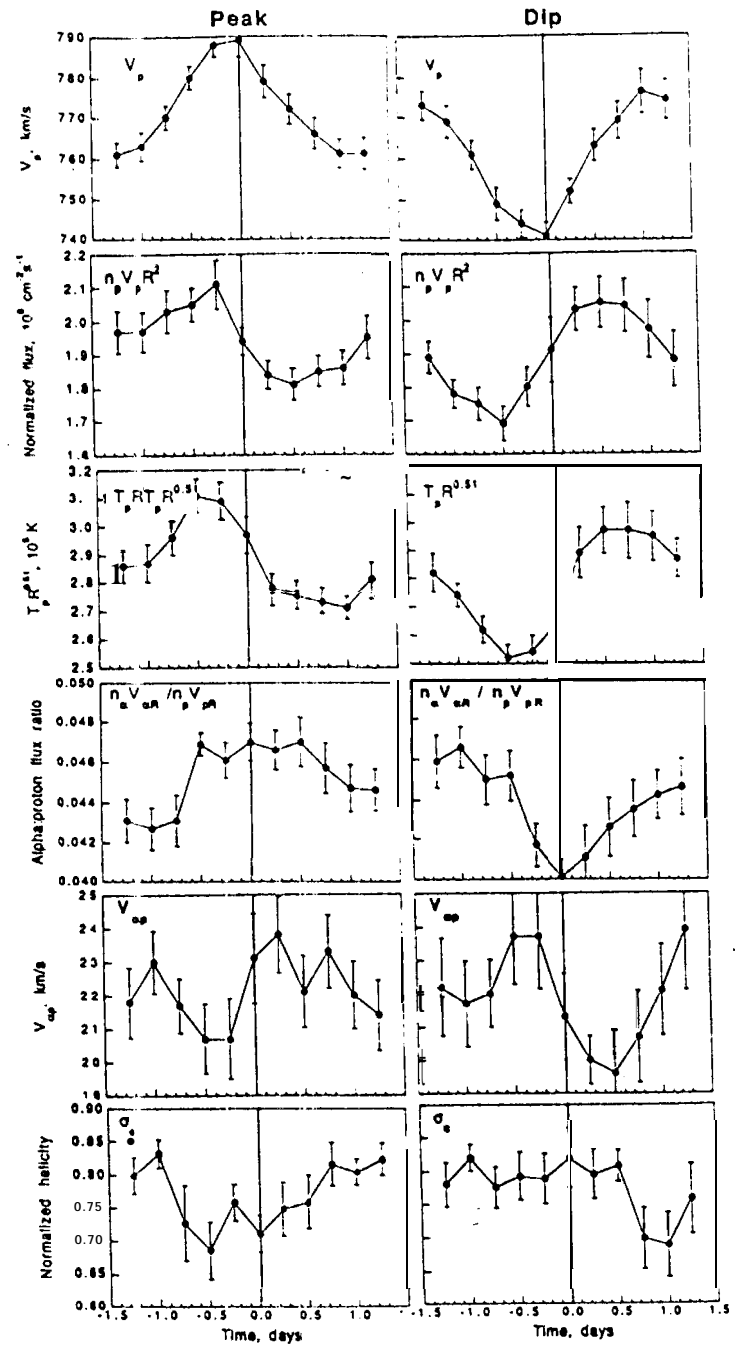


Fig 4

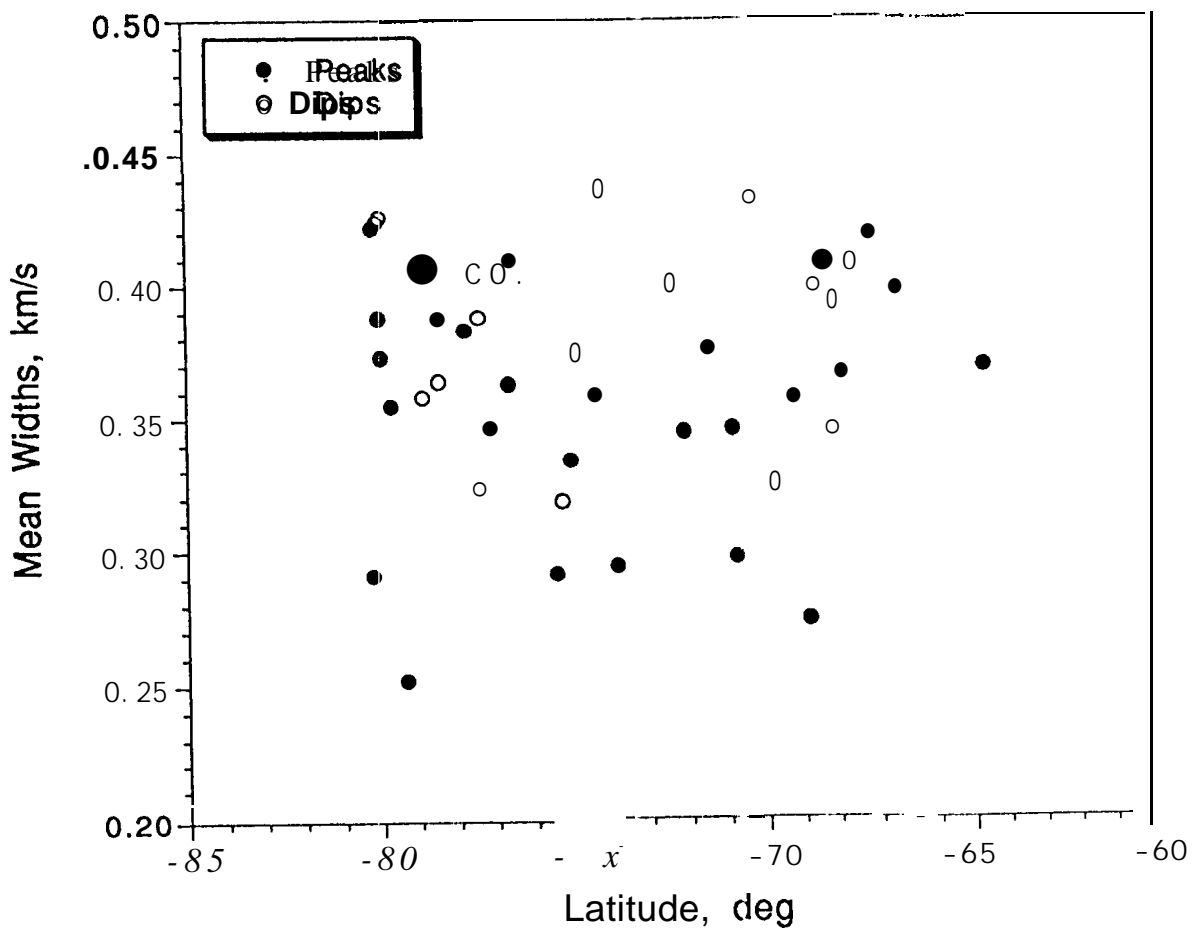


Fig 5

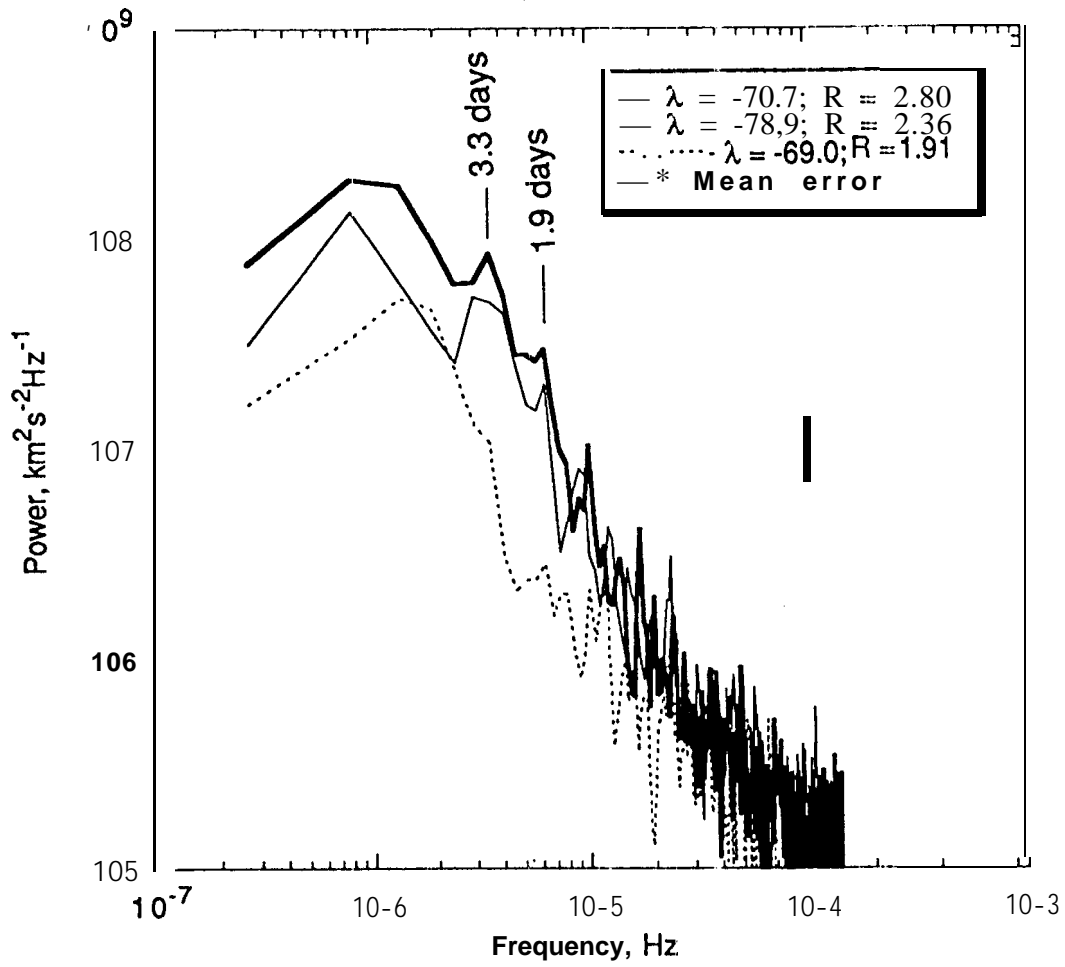


Fig 6